

Cosmological Dynamics in Interacting Scalar-Torsion $f(T, \phi)$ Gravity: Investigating Energy and Momentum Couplings

Carlos Rodriguez-Benites,^{1, 2, *} Manuel Gonzalez-Espinoza,^{3, †} Giovanni Otalora,^{4, ‡} and Manuel Alva-Morales^{2, 5, §}

¹*Departamento Académico de Física, Facultad de Ciencias Físicas y Matemáticas,
Universidad Nacional de Trujillo, Av. Juan Pablo II s/n, Trujillo, Perú*

²*GRACOCC & OASIS research groups, Facultad de Ciencias Físicas y Matemáticas,
Universidad Nacional de Trujillo, Av. Juan Pablo II s/n, Trujillo, Perú*

³*Laboratorio de Didáctica de la Física, Departamento de Matemática, Física y Computación,
Facultad de Ciencias Naturales y Exactas, Universidad de Playa Ancha,
Subida Leopoldo Carvallo 270, Valparaíso, Chile.*

⁴*Departamento de Física, Facultad de Ciencias, Universidad de Tarapacá, Casilla 7-D, Arica, Chile*

⁵*Escuela Profesional de Física, Facultad de Ciencias Físicas y Matemáticas,
Universidad Nacional de Trujillo, Av. Juan Pablo II s/n, Trujillo, Perú*

(Dated: August 28, 2024)

We investigate the cosmological dynamics of a homogeneous scalar field non-minimally coupled to torsion gravity, which also interacts with cold dark matter through energy and momentum transfer. The matter and radiation perfect fluids are modeled using the Sorkin-Schutz formalism. We identify scaling regimes of the field during both the radiation and matter eras. Additionally, we discovered a field-dominated scaling attractor; however, it does not exhibit accelerated expansion, making it unsuitable for describing dark energy. Nevertheless, we find two attractor solutions that do exhibit accelerated expansion: one is a quintessence-like fixed point, and the other is a de Sitter fixed point.

PACS numbers: 04.50.Kd, 98.80.-k, 95.36.+x

I. INTRODUCTION

In 1998, the analysis of Type Ia supernova (SNIa) data revealed that our Universe is expanding at an accelerating rate [1, 2]. Despite this discovery, there is no definitive explanation for this phenomenon. The prevailing interpretation attributes this accelerated expansion to dark energy, which could be a new form of exotic matter or a modification to gravity. Dark energy is believed to constitute 68% of the Universe's matter-energy density [3, 4]. While standard cosmology based on Einstein's General Relativity has successfully explained this acceleration through the cosmological constant Λ , the Λ CDM model (cosmological constant Λ and cold dark matter) faces a severe fine-tuning problem related to its energy scale [5–8]. Additionally, recent analyses have identified statistically significant tensions within the Λ CDM model, such as the H_0 discrepancy between the cosmic microwave background (CMB) measurements and direct local distance ladder measurements [9–12], as well as tensions involving the matter energy density Ω_m and the structure growth rate ($f\sigma_8$) [13–17]. These tensions suggest the need for investigating new physics beyond the standard cosmological model [18–24].

A promising alternative to explain dark energy is through scalar fields, which have been extensively studied in the literature. This includes models such as

quintessence [25–28], k-essence [29–31], and tachyon fields [32, 33], among others [7, 8]. From the perspective of quantum field theory in curved spacetime, a non-minimal coupling to gravity can naturally arise through quantum corrections [34] or renormalizability requirements [35–37]. For example, the extended quintessence model, which involves a quintessence field coupled to gravity, was first proposed in [38] and further explored in [39–44]. Similarly, non-minimally coupled k-essence and tachyonic fields have been investigated in [45] and [46], respectively. Galileon models also benefit from a non-minimal coupling to curvature, which helps avoid pathological instabilities or the propagation of additional degrees of freedom [47]. Recent studies have shown that non-minimally coupled scalar field theories can alleviate current observational tensions within the concordance model [19, 48].

Teleparallel Gravity (TG) offers an equivalent description of gravity through torsion rather than curvature [49–60]. In TG, the tetrad fields replace the metric tensor, and the Weitzenböck connection replaces the Levi-Civita connection [57–60]. The TG Lagrangian density is proportional to the torsion scalar T , which differs from the curvature scalar R by a total derivative term, making the two theories equivalent at the field equations level [59, 61]. Extending TG to include a non-minimally coupled scalar-torsion theory leads to models like the one proposed in [62, 63], where a scalar field ϕ is coupled to the torsion scalar T via a term $\xi\phi^2T$. This model was first applied to dark energy in [64, 65] and further extended in [66, 67]. Unlike the curvature-based theories, these scalar-torsion theories belong to a distinct class of gravitational modifications.

* cerodriguez@unitru.edu.pe

† manuel.gonzalez@upla.cl

‡ giovanni.otalora@academicos.uta.cl

§ malvam@unitru.edu.pe

Further generalizations involve introducing terms in the form $F(\phi)G(T)$ in the action, where $G(T)$ is a function of the torsion scalar T , or considering a general function $f(T, \phi)$ [68–70]. These modifications can also include a non-minimal coupling between the torsion scalar and matter fields [71–74], similar to the curvature-matter coupling in $f(R)$ gravity [75–83]. These theories are motivated by counterterms that appear during the quantization of self-interacting scalar fields in curved spacetime [84]. For example, a generalized scalar-torsion $f(T, \phi)$ gravity theory has been shown to be necessary for explaining primordial fluctuations during slow-roll inflation [85]. For dark energy at late times, these theories demonstrate new scaling solutions and attractor fixed points with accelerated expansion [7, 8, 86–94].

While these modified gravity theories can account for the observed accelerated expansion at late times and early inflation, they introduce at least one additional degree of freedom. It is crucial to ensure that the evolution of these modes does not result in pathological instabilities such as ghost, Laplacian, or tachyonic instabilities [95–99]. At the perturbation level, these additional modes are coupled to those of the matter fields, necessitating a complete stability analysis that includes matter interactions [100, 101].

Interacting scenarios between dark matter and dark energy appear as candidates to solve or alleviate the cosmological coincidence problem and have been widely studied, mainly through a phenomenological interaction kernel, which has been shown to affect the evolution of the Universe [102–106]. The interaction kernel may also provide a momentum exchange between the dark components, and it has been studied in alternative descriptions of the matter sector [107–112]. In this context, the Sorkin-Schutz action provides a framework to describe the matter sector, allowing for a comprehensive stability analysis in the presence of matter [113–115]. This analysis is essential for determining the viability of the theory before it can be compared with observational data [95, 96].

This paper is organized as follows: In section II, we briefly introduce the basic elements of teleparallel gravity. In Section III, we establish the general action to be studied. We develop the phase space analysis for the FLRW universe, obtaining the critical points and stability conditions. In Section IV, we numerically integrate the full cosmological equations using the dynamical analysis approach, corroborating the analytical results obtained in the previous sections. Finally, in Section V, we summarize the results obtained.

II. AN OVERVIEW OF TELEPARALLEL GRAVITY

The Teleparallel Equivalent of General Relativity, also called Teleparallel Gravity (TG), is a gauge theory for the translation group [55–57, 59–61], in which the dynamical

variable is the tetrad field that satisfies

$$g_{\mu\nu} = \eta_{AB} e_\mu^A e_\nu^B, \quad (1)$$

where $g_{\mu\nu}$ is the spacetime metric, and $\eta_{AB} = \text{diag}(-1, 1, 1, 1)$ is the Minkowski tangent space metric.

The Lorentz (or spin) connection of TG is defined as

$$\omega^A_{B\mu} = \Lambda^A_D(x) \partial_\mu \Lambda_B^D(x), \quad (2)$$

where $\Lambda^A_D(x)$ are the components of a local (point-dependent) Lorentz transformation. For this connection one has a vanishing curvature tensor

$$R^A_{B\mu\nu} = \partial_\mu \omega^A_{B\nu} - \partial_\nu \omega^A_{B\mu} + \omega^A_{C\mu} \omega^C_{B\nu} - \omega^A_{C\nu} \omega^C_{B\mu} = 0, \quad (3)$$

while in the presence of gravity this provides us with a non-vanishing torsion tensor

$$T^A_{\mu\nu} = \partial_\mu e^A_\nu - \partial_\nu e^A_\mu + \omega^A_{B\mu} e^B_\nu - \omega^A_{B\nu} e^B_\mu. \quad (4)$$

Due to these properties, this connection is called a purely inertial connection or simply flat connection.

Additionally, one can construct a spacetime-indexed linear connection, the so called Weitzenböck connection, in the form

$$\Gamma^\rho_{\nu\mu} = e_A^\rho \partial_\mu e^A_\nu + e_A^\rho \omega^A_{B\mu} e^B_\nu. \quad (5)$$

By introducing the contortion tensor

$$K^\rho_{\nu\mu} = \frac{1}{2} (T^\rho_{\nu\mu} + T^\rho_{\mu\nu} - T^\rho_{\nu\mu}), \quad (6)$$

where $T^\rho_{\mu\nu} = e_A^\rho T^A_{\mu\nu}$ is the purely spacetime form of the torsion tensor, that the Weitzenböck connection satisfies the general relation

$$\Gamma^\rho_{\nu\mu} = \bar{\Gamma}^\rho_{\nu\mu} + K^\rho_{\nu\mu}, \quad (7)$$

where $\bar{\Gamma}^\rho_{\nu\mu}$ is the known Levi-Civita connection of GR, and such that

$$T^\rho_{\mu\nu} = \Gamma^\rho_{\nu\mu} - \Gamma^\rho_{\mu\nu}. \quad (8)$$

Given its foundations as a gauge theory, the action of TG is constructed using quadratic terms in the torsion tensor [61]

$$S = -\frac{1}{2\kappa^2} \int d^4x e T, \quad (9)$$

where $e = \det\{(e^A_\mu)\} = \sqrt{-g}$ and T is the torsion scalar such that

$$T = S_\rho^{\mu\nu} T^\rho_{\mu\nu}, \quad (10)$$

with

$$S_\rho^{\mu\nu} = \frac{1}{2} \left(K^{\mu\nu}_\rho + \delta^\mu_\rho T^{\theta\nu}_\theta - \delta^\nu_\rho T^{\theta\mu}_\theta \right), \quad (11)$$

the super-potential tensor.

Putting Eq. (7) into (10), one can show that

$$T = -R + 2e^{-1}\partial_\mu(eT^{\nu\mu})_\nu, \quad (12)$$

where R is the curvature scalar of GR. Since T and R differ by a total derivative term, the two theories, TG and GR, are equivalent at the level of field equations.

Alternatively, modified gravity models can be developed from either curvature-based or torsion-based theories, which may lead to non-equivalent results. In the context of modified teleparallel gravity, various studies have examined dark energy and inflation driven by non-minimally coupled scalar fields [64, 66, 67, 116, 117]. Additionally, models incorporating non-linear torsion terms, like $f(T)$ gravity [68, 69], have been explored [70, 74]. These torsion-based theories, distinct from curvature-based ones, have led to extensive research in early and late-time cosmology [62].

III. INTERACTING SCALAR-TORSION $f(T, \phi)$ GRAVITY

The relevant action is constructed from the scalar-torsion $f(T, \phi)$ gravity action [85, 86, 115, 118] by incorporating interactions that involve energy and momentum transfer between the scalar field and cold dark matter [119]. This is achieved using the Sorkin-Schutz formalism [113, 114], as follows:

$$S = \int d^4x e [f(T, \phi) - f_1(\phi, X, Z)\rho_m + f_2(\phi, X, Z)] - \sum_{j=m,r} \int d^4x [e\rho_j(n) + J_j^\nu \partial_\nu \ell_j], \quad (13)$$

where $f(T, \phi)$ is an arbitrary function of the torsion scalar T , and the scalar field ϕ , with $X = -\nabla^\mu \phi \nabla_\mu \phi/2$ as its kinetic term. The variable $Z = u^\mu \nabla_\mu \phi$ is a scalar combination involving the field derivative coupling with the fluid four velocity u^μ .

The interaction between the scalar field and cold dark matter fluid is introduced through the functions f_1 and f_2 , both of which depend on ϕ , X , and Z . The function f_1 provides the energy transfer, while f_2 accounts for both momentum exchange and the scalar potential [107].

The second integral in (13) is the Sorkin-Schutz action describing both matter and radiation fluids. In this context, n denotes the number density, and J^ν is the current vector field. The variable ℓ is a Lagrange multiplier that leads to the conservation of J^ν [107, 108].

A. Cosmological dynamics

In this section, we explore the cosmological dynamics of this model by introducing the cosmological background and useful cosmological parameters. To analyze cosmology within this interacting model, we define the

cosmological background by assuming a diagonal tetrad field:

$$e_\mu^A = \text{diag}(1, a, a, a), \quad (14)$$

which corresponds to the Friedmann-Lemaître-Robertson-Walker (FLRW) spacetime metric with flat spacelike sections

$$ds^2 = -dt^2 + a^2 \delta_{ij} dx^i dx^j, \quad (15)$$

where a is the scale factor which is a function of the cosmic time t only. Hence, the background equations are given by

$$\begin{aligned} f - 2Tf_{,T} - f_1\rho_m + \rho_m f_{1,X}\dot{\phi}^2 + \rho_m f_{1,Z}\dot{\phi} \\ + f_2 - f_{2,X}\dot{\phi}^2 - f_{2,Z}\dot{\phi} = \rho_m + \rho_r, \end{aligned} \quad (16)$$

$$f - 2Tf_{,T} - 4\dot{H}f_{,T} - 4H\dot{f}_{,T} + f_2 = -p_r, \quad (17)$$

$$\begin{aligned} (-\rho_m f_{1,ZZ} - \rho_m f_{1,X} - 2\dot{\phi}\rho_m f_{1,XZ} - 2X\rho_m f_{1,XX} \\ + f_{2,ZZ} + f_{2,X} + 2\dot{\phi}f_{2,XZ} + 2Xf_{2,XX})\ddot{\phi} \\ + 3H(\dot{\phi}f_{2,X} + f_{2,Z}) + \rho_m f_{1,\phi} - f_{2,\phi}\dot{\phi}f_{2,\phi Z} - \dot{\phi}\rho_m f_{1,\phi Z} \\ 2Xf_{2,\phi X} - 2X\rho_m f_{1,\phi X} - f_{,\phi} = 0, \end{aligned} \quad (18)$$

where $H \equiv \dot{a}/a$ is the Hubble rate, a dot represents derivative with respect to t , and a comma denotes derivative with respect to ϕ , X , Z or T .

Then, by using the following definitions for the arbitrary functions f , f_1 and f_2 [107]:

$$f = -\frac{1}{2\kappa^2}T - \frac{F(\phi)T}{6}, \quad (19)$$

$$f_1 = \frac{1}{V_2(\phi)} - 1, \quad (20)$$

$$f_2 = X \left[1 - \frac{1}{Y_1} + 2^{1-s/2}\beta \left(\frac{Y_2^s}{Y_1^{s/2}} \right) \right], \quad (21)$$

where $Y_1 = X/V_1(\phi)$ and $Y_2 = Z/\sqrt{V_1(\phi)}$, the background equations (16)-(18) become

$$\frac{3H^2}{\kappa^2} = -FH^2 + \beta\dot{\phi}^2 + \rho_r + V_1 + \tilde{\rho}_m + \frac{1}{2}\dot{\phi}^2, \quad (22)$$

$$\begin{aligned} -\frac{2\dot{H}}{\kappa^2} = \frac{2}{3}H\dot{\phi}F_{,\phi} + \frac{2}{3}F\dot{H} + 2\beta\dot{\phi}^2 + \frac{4}{3}\rho_r + \tilde{\rho}_m + \dot{\phi}^2, \end{aligned} \quad (23)$$

$$(1 + 2\beta)\ddot{\phi} + H^2 F_{,\phi} + 3H\dot{\phi}(2\beta + 1) + V_{1,\phi} - \frac{\tilde{\rho}_m V_{2,\phi}}{V_2} = 0, \quad (24)$$

where we have defined $\tilde{\rho}_m \equiv \rho_m/V_2$ as an effective matter energy density variable.

Following Ref. [7] one can rewrite the Friedmann equations (22) and (23) in their standard form as

$$\frac{3}{\kappa^2}H^2 = \rho_{de} + \tilde{\rho}_m + \rho_r, \quad (25)$$

$$-\frac{2}{\kappa^2}\dot{H} = \rho_{de} + p_{de} + \tilde{\rho}_m + \frac{4}{3}\rho_r, \quad (26)$$

where the effective energy and pressure densities are defined as

$$\rho_{de} = \left(\beta + \frac{1}{2}\right)\dot{\phi}^2 + V_1 - FH^2, \quad (27)$$

$$p_{de} = \frac{2}{3}H\dot{\phi}F_{,\phi} + \frac{2}{3}F\dot{H} + FH^2 + \left(\beta + \frac{1}{2}\right)\dot{\phi}^2 - V_1. \quad (28)$$

Then, the effective dark energy equation-of-state (EOS) parameter is

$$w_{de} = \frac{p_{de}}{\rho_{de}}. \quad (29)$$

For these definitions of ρ_{de} and p_{de} one can verify that they satisfy

$$\dot{\rho}_{de} + 3H(\rho_{de} + p_{de}) = -\rho_m\dot{f}_1. \quad (30)$$

This equation is consistent with the energy conservation law and the fluid evolution equations

$$\dot{\tilde{\rho}}_m + 3H\tilde{\rho}_m = +\rho_m\dot{f}_1, \quad (31)$$

$$\dot{\rho}_r + 4H\rho_r = 0. \quad (32)$$

It is also useful to introduce the total equation of state (EoS) parameter as

$$w_{\text{tot}} = \frac{p_{de} + p_r}{\rho_{de} + \tilde{\rho}_m + \rho_r}, \quad (33)$$

which is related to the deceleration parameter q through

$$q = \frac{1}{2}(1 + 3w_{\text{tot}}). \quad (34)$$

Thus, the Universe undergoes acceleration for $q < 0$, or equivalently for $w_{\text{tot}} < -\frac{1}{3}$.

Finally, another useful set of cosmological parameters we can introduce is the standard density parameters:

$$\Omega_m \equiv \frac{\kappa^2\tilde{\rho}_m}{3H^2}, \quad \Omega_{de} \equiv \frac{\kappa^2\rho_{de}}{3H^2}, \quad \Omega_r \equiv \frac{\kappa^2\rho_r}{3H^2}, \quad (35)$$

which satisfies the constraint equation

$$\Omega_{de} + \Omega_m + \Omega_r = 1. \quad (36)$$

This equation constrains the energy density of each component of the Universe in the same way as the Friedmann equation (25), but expressed in terms of the density parameters.

A detailed dynamical analysis of this model is performed in the following section, where we construct the corresponding dynamical system from equations (25), (26), (31), and (32).

B. Phase space Analysis

In order to obtain the dynamical system of the model, we introduce the following set of dimensionless variables [7]:

$$\begin{aligned} x &= \frac{\kappa\dot{\phi}}{\sqrt{6}H}, & y &= \frac{\kappa\sqrt{V_1}}{\sqrt{3}H}, & u &= -\frac{1}{3}\kappa^2F, \\ \Omega_m &= \frac{\kappa^2\rho_m}{V_2 3H^2}, & \lambda &= -\frac{V_{1,\phi}}{\kappa V_1}, & \sigma &= -\frac{F_{,\phi}}{\kappa F}, \\ Q &= -\frac{V_{2,\phi}}{\kappa V_2}, & \Theta &= \frac{FF_{,\phi\phi}}{(F_{,\phi})^2}, & \Gamma_1 &= \frac{V_1 V_{1,\phi\phi}}{(V_{1,\phi})^2}, \\ \Gamma_2 &= \frac{V_2 V_{2,\phi\phi}}{(V_{2,\phi})^2}, & \varrho &= \frac{\kappa\sqrt{\rho_r}}{\sqrt{3}H}, \end{aligned} \quad (37)$$

and the constraint equation

$$\Omega_m + \varrho^2 + u + (1 + 2\beta)x^2 + y^2 = 1. \quad (38)$$

Therefore, we obtain the dynamical system

$$\frac{dx}{dN} = F_1(x, y, \varrho, u, \lambda, Q, \sigma), \quad (39)$$

$$\frac{dy}{dN} = \frac{1}{2(u-1)}F_2(x, y, \varrho, u, \lambda, Q, \sigma), \quad (40)$$

$$\frac{d\varrho}{dN} = -\frac{\varrho F_3(x, y, \varrho, u, \lambda, Q, \sigma)}{2(u-1)}, \quad (41)$$

$$\frac{du}{dN} = -\sqrt{6}\sigma xu, \quad (42)$$

$$\frac{d\lambda}{dN} = -\sqrt{6}(\Gamma_1 - 1)\lambda^2x, \quad (43)$$

$$\frac{dQ}{dN} = -\sqrt{6}(\Gamma_2 - 1)Q^2x, \quad (44)$$

$$\frac{d\sigma}{dN} = -\sqrt{6}(\Theta - 1)\sigma^2x, \quad (45)$$

where,

$$\begin{aligned} F_1 &= \frac{1}{2} \left[\frac{\sqrt{6}(Q((2\beta+1)x^2 + y^2 + u + \varrho^2 - 1) + \lambda y^2 - \sigma u)}{2\beta+1} \right. \\ &\quad \left. - \frac{3(2\beta+1)x^3 - 2\sqrt{6}\sigma x^2u - x(-3y^2 + 3u + \varrho^2 - 3)}{u-1} \right], \end{aligned}$$

$$\begin{aligned} F_2 &= y \left[\sqrt{6}x(\lambda - \lambda u - 2\sigma u) + 3u - 3(2\beta+1)x^2 + \right. \\ &\quad \left. + 3y^2 - \varrho^2 - 3 \right], \end{aligned}$$

$$F_3 = (6\beta+3)x^2 + 2\sqrt{6}\sigma xu - 3y^2 + u + \varrho^2 - 1.$$

Using the above set of phase space variables, we can

Table I. Critical points for the autonomous system.

Name	x_c	y_c	u_c	ϱ_c
a_R	0	0	0	1
b	0	$\sqrt{\frac{\sigma}{\lambda + \sigma}}$	$\frac{\lambda}{\lambda + \sigma}$	0
c_R	$-\frac{1}{\sqrt{6}Q}$	0	0	$\frac{\sqrt{Q^2 - \beta - \frac{1}{2}}}{Q}$
d_M	$-\sqrt{\frac{2}{3}} \frac{Q}{1 + 2\beta}$	0	0	0
e^\pm	$\pm \frac{1}{\sqrt{1 + 2\beta}}$	0	0	0
f_R	$\sqrt{\frac{2}{3}} \frac{2}{\lambda}$	$\sqrt{\frac{1 + 2\beta}{3}} \frac{2}{\lambda}$	0	$\frac{\sqrt{\lambda^2 - 8\beta - 4}}{\lambda}$
g	$\frac{\lambda}{\sqrt{6}(1 + 2\beta)}$	$\sqrt{\frac{6 + 12\beta - \lambda^2}{6(1 + 2\beta)}}$	0	0
h	$\sqrt{\frac{3}{2}} \frac{1}{Q + \lambda}$	$\frac{\sqrt{3 + 2Q^2 + 6\beta + 2Q\lambda}}{\sqrt{2}(Q + \lambda)}$	0	0
i_M	0	0	$\frac{Q}{Q - \sigma}$	0

also write

$$\Omega_{de} = (1 + 2\beta)x^2 + y^2 + u, \quad (46)$$

$$\Omega_m = 1 - (1 + 2\beta)x^2 - y^2 - u - \varrho^2, \quad (47)$$

$$\Omega_r = \varrho^2. \quad (48)$$

Similarly, the equation of state of dark energy $w_{de} = p_{de}/\rho_{de}$ can be rewritten as

$$w_{de} = -\frac{2\sqrt{6}\sigma ux + u\varrho^2 + (6\beta + 3)x^2 - 3y^2}{3(u - 1)[u + (2\beta + 1)x^2 + y^2]}, \quad (49)$$

whereas the total equation of state becomes

$$w_{tot} = \frac{1}{3} \left[\varrho^2 - \frac{2\sqrt{6}\sigma ux + u\varrho^2 + (6\beta + 3)x^2 - 3y^2}{u - 1} \right]. \quad (50)$$

For the dynamical system described by (39)-(42) to be autonomous, the parameters Γ_1 , Γ_2 , and Θ must be known. Therefore, we select the following exponential functions: $V_1 \sim e^{-\kappa\lambda\phi}$, $V_2 \sim e^{-\kappa Q\phi}$, and $F \sim e^{-\kappa\sigma\phi}$. In this way we set the values $\Gamma_1 = \Gamma_2 = \Theta = 1$ and establish λ , Q and σ as dimensionless constants for the

model. These types of functions have been shown to lead to accelerated expansion and the derivation of scaling solutions in previous works [7, 8, 107, 120].

C. Critical points

In this section, we obtain the critical points from the conditions $dx/dN = dy/dN = d\varrho/dN = du/dN = 0$, considering $V_1 \sim e^{-\kappa\lambda\phi}$, $V_2 \sim e^{-\kappa Q\phi}$ and $F \sim e^{-\kappa\sigma\phi}$ [7, 119]. Where we consider the definition of each dynamical variable (37) and that the physically allowable critical points are given by $y_c \geq 0$, $\varrho_c \geq 0$ and $u_c \geq 0$. The critical points of the system (39)-(42) are shown in Table I and the values of their cosmological parameters in Table II. Also, in this subsection and further on, we introduce the parameters $\Omega_{de}^{(r)}$ and $\Omega_{de}^{(m)}$, representing the fractional density of dark energy during the radiation-dominated and dark matter-dominated eras, respectively. The conditions of existence and acceleration associated with the parameters of each critical point are presented in Table III.

The critical point a_R corresponds to a radiation with $\Omega_r = 1$ and $w_{de} = w_{tot} = 1/3$. Point b is a de Sitter solution with $\Omega_{de} = 1$, and $w_{de} = w_{tot} = -1$, which

Table II. Cosmological parameters for the critical points shown in Table I

Name	Ω_{de}	Ω_m	Ω_r	w_{de}	w_{tot}
a_R	0	0	1	$\frac{1}{3}$	$\frac{1}{3}$
b	1	0	0	-1	-1
c_R	$\frac{1+2\beta}{6Q^2}$	$\frac{1+2\beta}{3Q^2}$	$1 - \frac{1+2\beta}{2Q^2}$	1	$\frac{1}{3}$
d_M	$\frac{2Q^2}{6\beta+3}$	$\frac{6\beta-2Q^2+3}{6\beta+3}$	0	1	$\frac{2Q^2}{6\beta+3}$
e^\pm	1	0	0	1	1
f_R	$\frac{8\beta+4}{\lambda^2}$	0	$1 - \frac{8\beta+4}{\lambda^2}$	$\frac{1}{3}$	$\frac{1}{3}$
g	1	0	0	$\frac{\lambda^2}{6\beta+3} - 1$	$\frac{\lambda^2}{6\beta+3} - 1$
h	$\frac{6\beta+Q^2+\lambda Q+3}{(\lambda+Q)^2}$	$\frac{-6\beta+\lambda^2+\lambda Q-3}{(\lambda+Q)^2}$	0	$-\frac{Q(\lambda+Q)}{6\beta+Q(\lambda+Q)+3}$	$-\frac{Q}{\lambda+Q}$
i_M	$\frac{Q}{Q-\sigma}$	$1 - \frac{Q}{Q-\sigma}$	0	0	0

provides accelerated expansion for all values of the parameters. Critical point c_R represents a scaling radiation era, for which $\Omega_{de}^{(r)} = (1+2\beta)/6Q^2$, $w_{de} = 1$, and $w_{tot} = 1/3$. It should satisfy the early constraint imposed by the physics of Big Bang Nucleosynthesis (BBN), ensuring $\Omega_{de}^{(r)} < 0.045$ [121, 122].

On the other hand, for $Q = 0$, the critical point d_M represents a matter-dominated era with $\Omega_m = 1$, $w_{de} = 1$, and $w_{tot} = 0$. For $Q \neq 0$, we have a scaling matter era with $\Omega_{de} = 2Q^2/(6\beta+3)$, which is constrained to satisfy $\Omega_{de}^{(m)} < 0.02$ (95% C.L.), at redshift $z \approx 50$, according to CMB measurements [4]. In both cases of Q , dark energy behaves like stiff matter with $w_{de} = 1$. Since $w_{tot} = 2Q^2/(6\beta+3)$, this point presents acceleration for $-(1+2Q^2)/2 < \beta < -1/2$.

Point e^\pm is a dark energy dominated solution which satisfies $\Omega_{de} = 1$, but it cannot explain the current accelerated expansion due to its behavior as stiff matter with $w_{de} = w_{tot} = 1$.

The critical point f_R corresponds to a scaling radiation era, where $\Omega_{de}^{(r)} = 1 - (8\beta+4)/\lambda^2$. Therefore, it should satisfy the early constraint imposed by the physics of BBN, ensuring $\Omega_{de}^{(r)} < 0.045$ [121, 122]. It is worth noting that dark energy behaves as a radiation fluid with $w_{de} = w_{tot} = 1/3$.

Point g provides a dark energy-dominated era, which can explain the cosmic accelerated expansion when $w_{tot} < -1/3$.

The point labeled as h represents a matter-scaling era. As shown in Table II, for this fixed point, the values of the cosmological parameters depend on both the energy and momentum couplings. This point is constrained to satisfy $\Omega_{de}^{(m)} < 0.02$ (95% C.L.), at redshift de $z \approx 50$, according to CMB measurements [4]. In the case where $Q = 0$ satisfies $w_{de} = w_{tot} = 0$, behaving as cold dark matter. For $Q \neq 0$, this fixed point can provide accelerated expansion and domination of dark energy over matter.

Finally, point i_M represents a matter-scaling era, characterized by $\Omega_{de} = Q/(Q-\sigma)$, $\Omega_m = 1 - Q/(Q-\sigma)$, and $w_{de} = w_{tot} = 0$. As noted, these values depend on both the energy coupling Q and the non-minimal coupling to gravity σ .

In the following section, we will examine the stability conditions for these critical points. These conditions are determined through a linear analysis of perturbations in the phase space variables.

D. Stability

To determine the stability of critical points, we perturb the autonomous system (39)-(45) using linear perturbations δx , δy , $\delta \varrho$, and δu . The stability of each critical point is determined by examining the sign of the eigenvalues μ of the four-dimensional Jacobian matrix evaluated at each critical point [7].

- Point a_R has the eigenvalues

$$\mu_1 = -1, \mu_2 = 1, \mu_3 = 0, \mu_4 = 2. \quad (51)$$

- Point b has the eigenvalues

$$\begin{aligned} \mu_1 &= -3, \mu_2 = -2, \\ \mu_{3,4} &= -\frac{3+6\beta \pm \sqrt{3(1+2\beta)(3+6\beta+4\lambda\sigma)}}{2+4\beta}. \end{aligned} \quad (52)$$

- Point c_R has the eigenvalues

$$\begin{aligned} \mu_{1,2} &= \frac{1}{2} \left[-1 \mp \sqrt{\frac{2-3Q^2+4\beta}{Q^2}} \right], \mu_3 = 2 + \frac{\lambda}{2Q}, \\ \mu_4 &= \frac{\sigma}{Q}. \end{aligned} \quad (53)$$

- Point d_M has the eigenvalues

$$\begin{aligned} \mu_1 &= -\frac{1}{2} + \frac{Q^2}{1+2\beta}, \mu_2 = -\frac{3}{2} + \frac{Q^2}{1+2\beta}, \\ \mu_3 &= \frac{2Q\sigma}{1+2\beta}, \mu_4 = \frac{3+6\beta+2Q(Q+\lambda)}{2+4\beta}. \end{aligned} \quad (54)$$

- Point e^\pm has the eigenvalues

$$\begin{aligned} \mu_1 &= 1, \mu_2 = 3 + \frac{\sqrt{6}Q}{\sqrt{1+2\beta}}, \\ \mu_3 &= 3 - \frac{\sqrt{3}\lambda}{\sqrt{2(1+2\beta)}}, \mu_4 = -\frac{\sqrt{6}\sigma}{\sqrt{1+2\beta}}. \end{aligned} \quad (55)$$

- Point f_R has the eigenvalues

$$\begin{aligned} \mu_1 &= 1 + \frac{4Q}{\lambda}, \mu_2 = -\frac{4\sigma}{\lambda}, \\ \mu_{3,4} &= -\frac{\lambda \pm \sqrt{64+128\beta-15\lambda^2}}{2\lambda}. \end{aligned} \quad (56)$$

- Point g has the eigenvalues

$$\begin{aligned} \mu_1 &= -3 + \frac{\lambda^2}{2+4\beta}, \mu_2 = \frac{-3-6\beta+\lambda(Q+\lambda)}{1+2\beta}, \\ \mu_3 &= -2 + \frac{\lambda^2}{2+4\beta}, \mu_4 = -\frac{\lambda\sigma}{1+2\beta}. \end{aligned} \quad (57)$$

- Point h has the eigenvalues

$$\begin{aligned} \mu_1 &= -\frac{4Q+\lambda}{2(Q+\lambda)}, \mu_2 = -\frac{3\sigma}{Q+\lambda}, \\ \mu_{3,4} &= -\frac{1}{4} \left[-6 + \frac{3\lambda}{Q+\lambda} \pm \right. \\ &\quad \left. \sqrt{-63 - \frac{48Q\lambda}{1+2\beta} + \frac{9(24+Q^2+48\beta)}{(Q+\lambda)^2} + \frac{234Q}{Q+\lambda}} \right] \end{aligned} \quad (58)$$

- Point i_M has the eigenvalues

$$\begin{aligned} \mu_1 &= -\frac{1}{2}, \mu_2 = \frac{3}{2}, \\ \mu_{3,4} &= \frac{1}{4} \left[-3 \mp \sqrt{9 - \frac{48Q\sigma}{1+2\beta}} \right]. \end{aligned} \quad (59)$$

Table III presents a detailed description of the stability conditions for each critical point, its corresponding eigenvalues, and the parameter constraints.

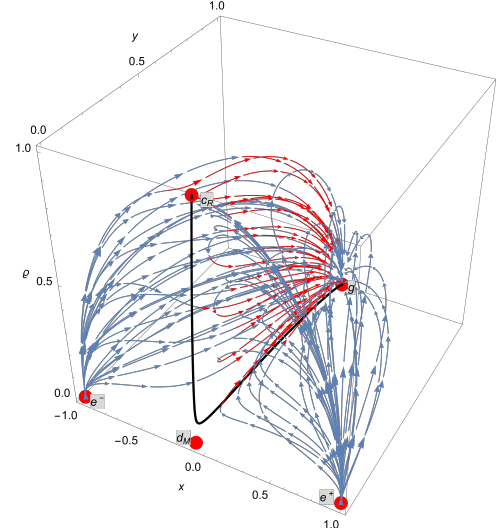


Fig. 1. Phase space stream plot for the values $\beta = 0.01$, $Q = 0.1$, $\lambda = 0.1$ and $\sigma = 0.1$. The black-solid curve corresponds to the evolution curve and represents the physical trajectory of the three-dimensional system with initial conditions $x_0 = 10^{-11}$, $y_0 = 7.4 \times 10^{-13}$, $u_0 = 10^{-12}$ and $\varrho = 0.99983$.

IV. NUMERICAL ANALYSIS

In this section, we conduct a numerical analysis of the autonomous system (39)-(42). Our investigation examines how well our model explains the current accelerated expansion of the Universe and compares our predictions with the latest observational data on cosmological parameters.

Figures 1, 2, and 3 illustrate the phase space stream flow for the trajectories $c_R \rightarrow d_M \rightarrow g$, $a_R \rightarrow d_M \rightarrow g \rightarrow$

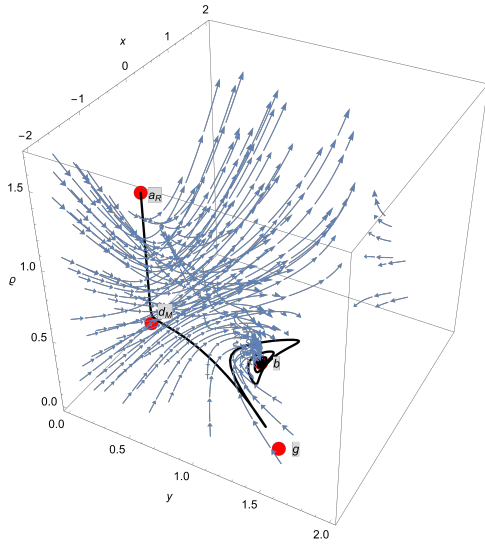


Fig. 2. Phase space stream plot for the values $\beta = -0.8$, $Q = -4.0 \times 10^{-3}$, $\lambda = 2$ and $\sigma = 17$. The black-solid curve corresponds to the evolution curve and represents the physical trajectory of the three-dimensional system with initial conditions $x_0 = 10^{-11}$, $y_0 = 4.9 \times 10^{-13}$, $u_0 = 10^{-12}$ and $\varrho = 0.99983$.

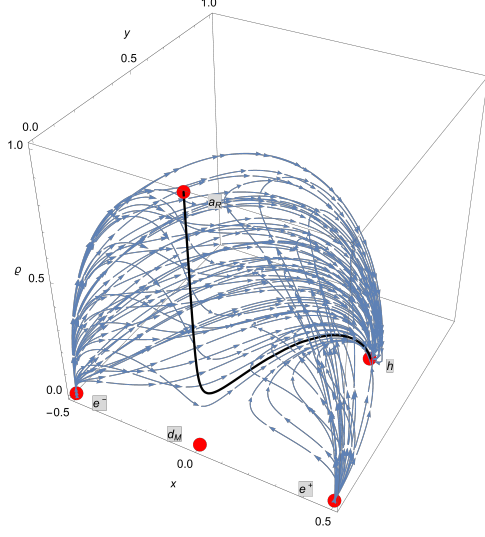


Fig. 3. Phase space stream plot for the values $\beta = 1.5$, $Q = 3.0 \times 10^{-2}$, $\lambda = 3.75$ and $\sigma = 1$. The black-solid curve corresponds to the evolution curve and represents the physical trajectory of the three-dimensional system with initial conditions $x_0 = 10^{-9}$, $y_0 = 5.1 \times 10^{-11}$, $u_0 = 10^{-9}$ and $\varrho = 0.99983$.

b , and $a_R \rightarrow d_M \rightarrow h$. It is evident that the solutions of the autonomous system converge to the attractors b and g , as well as to the new solution h for specific parameter values. Although the system exhibits a scaling attractor behavior, the primary physical trajectory of interest is $c_R \rightarrow d_M \rightarrow g$, highlighted by a red stream flow in Fig. 1.

In Fig. 4, we depict the behavior of the fractional en-

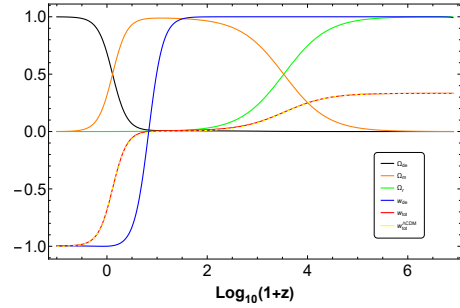


Fig. 4. We depict the evolution of the fractional energy of dark energy Ω_{de} (black), dark matter (including baryons) Ω_m (orange), radiation Ω_r (green), equation of state parameter of dark energy w_{de} (blue), total EoS parameter w_{tot} (red) and the EoS parameter of the Λ CDM model (yellow) as functions of the cosmological redshift, for the same initial conditions used in Fig. 1.

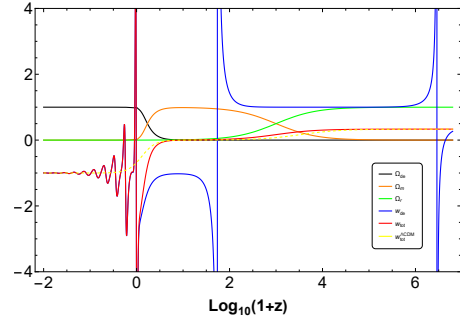


Fig. 5. We depict the evolution of the fractional energy of dark energy Ω_{de} (black), dark matter (including baryons) Ω_m (orange), radiation Ω_r (green), equation of state parameter of dark energy w_{de} (blue), total EoS parameter w_{tot} (red) and the EoS parameter of the Λ CDM model (yellow) as functions of the cosmological redshift, for the same initial conditions used in Fig. 2.

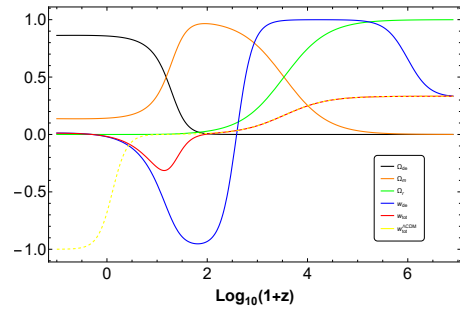


Fig. 6. We depict the evolution of the fractional energy of dark energy Ω_{de} (black), dark matter (including baryons) Ω_m (orange), radiation Ω_r (green), equation of state parameter of dark energy w_{de} (blue), total EoS parameter w_{tot} (red) and the EoS parameter of the Λ CDM model (yellow) as functions of the cosmological redshift, for the same initial conditions used in Fig. 3.

ergies of dark energy, matter (including baryons), and

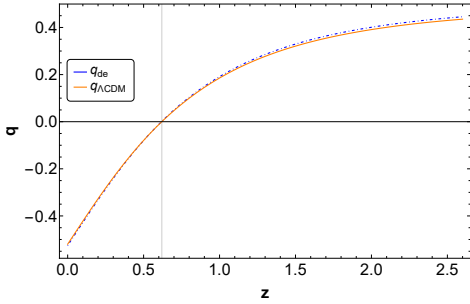


Fig. 7. We present the evolution of the deceleration parameter $q(z)$, calculated using the same initial conditions as those employed in Fig. 1. We also present the evolution curve of the deceleration parameter $q_{\Lambda\text{CDM}}(z)$ of the ΛCDM model.

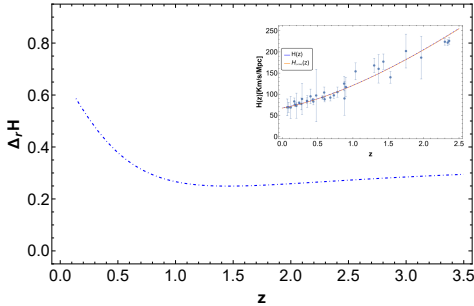


Fig. 8. We present the evolution of the Hubble rate $H(z)$ and its relative difference $\Delta_r H(z) = 100 \times \frac{|H - H_{\Lambda\text{CDM}}|}{H_{\Lambda\text{CDM}}}$ for the ΛCDM model as functions of redshift, using the same initial conditions depicted in Fig. 1. Additionally, we provide the evolution of the Hubble rate $H_{\Lambda\text{CDM}}$ within the ΛCDM framework, alongside observational Hubble data sourced from [123, 124]. The present-day Hubble rate, $H_0 = 67.4 \text{ km}/(\text{Mpc}\cdot\text{s})$, as reported by Planck 2018 [3], has been utilized in our analysis.

radiation, as well as the total EoS parameter and EoS parameter of dark energy for the physical trajectory $c_R \rightarrow d_M \rightarrow g$. The transition between the radiation and matter eras occurs around $z \approx 3387$, while the transition to the accelerated phase occurs around $z \approx 0.62$, as indicated by the deceleration parameter shown in Fig. 7. These values are very close to those predicted by the ΛCDM model and are consistent with current observational data [3]. Also, we have obtained the fractional energy density parameters of dark energy $\Omega_{de} \approx 0.68$ and matter $\Omega_m \approx 0.32$ with the equation of state of dark energy at $z = 0$ given by $w_{de}^{(0)} \approx -0.999392$, which is consistent with the observational constraint $w_{de}^{(0)} = -1.028 \pm 0.032$ from the latest observations [3]. We have also applied the constraint on the fractional energy density of dark energy during the scaling matter regime, derived from Planck CMB measurements, $\Omega_{de}^{(m)} < 0.02$ (95% C.L.) at a redshift of approximately $z \approx 50$ [4]. As shown in Fig. 4, we find $\Omega_{de}^{(m)} \approx 0.006$ at redshift $z = 50$ during the scaling matter era d_M .

Finally, in Fig. 8, we present an analysis of the Hubble rate (see Appendix B) by calculating the evolution of the Hubble rate $H(z)$ in our model, alongside the evolution of the Hubble rate $H_{\Lambda\text{CDM}}(z)$ for the ΛCDM model. This comparison uses the same parameter values and initial conditions as those in Fig. 1. The relative difference, $\Delta_r H(z)$, between our model and the ΛCDM model is also shown, demonstrating their close correspondence and consistent alignment with the latest observational data.

V. CONCLUDING REMARKS

We investigated the cosmological behavior of dark energy within a model that includes a scalar field non-minimally coupled to torsion gravity. This model also accounts for the interaction between the scalar field and cold dark matter through energy and momentum transfer. In this framework, torsion emerges from the Weitzenböck connection in teleparallel gravity, which is a flat connection that exhibits non-zero torsion in the presence of gravity. We derived the cosmological equations and formulated the corresponding autonomous system. A detailed phase space analysis was conducted, where we identified all critical points and determined their stability conditions. Additionally, we compared our theoretical predictions with the latest observational data from $H(z)$ measurements.

Our analysis identified a stable critical point, g , which corresponds to the current accelerated expansion of the Universe, resembling a quintessence-like fixed point. We also found a de Sitter attractor solution, b , which is a spiral stable point. This suggests that, regardless of the initial conditions—provided they are close to these attractor points—the system will naturally evolve toward a dark energy-dominated phase characterized by accelerated expansion. Additionally, we demonstrated that this late-time accelerated phase can be smoothly connected to the standard radiation and matter-dominated eras.

We also identified the presence of a matter-scaling era (d_M) associated with the interaction between dark energy and dark matter through the exchange of energy and momentum. Furthermore, we discovered a second fixed point, also a matter-scaling era (i_M), which arises due to the energy transfer from the scalar field to dark matter and its non-minimal coupling to gravity. Consequently, we determined the necessary conditions for the model parameters that allow the system to transition from these scaling regimes to a dark energy-dominated attractor with acceleration.

Finally, we obtained a scaling attractor solution (h) in which the energy density of the universe is dominated by the field density. These types of solutions are particularly interesting because they offer a natural mechanism for alleviating the coincidence problem [7]. However, in the context of the present model, this attractor solution is unable to simultaneously account for both the current

accelerated expansion and the thermal history of the universe.

ACKNOWLEDGMENTS

M. Gonzalez-Espinoza acknowledges the financial support of FONDECYT de Postdoctorado, N° 3230801. C.

Rodriguez-Benites and M. Alva-Morales acknowledge the financial support of PE501082885-2023-PROCIENCIA. G. Otalora gratefully acknowledges the hospitality of the *Institute of Cosmology and Gravitation (ICG)* at the University of Portsmouth, where part of this work was carried out.

-
- [1] A. G. Riess *et al.* (Supernova Search Team), Observational evidence from supernovae for an accelerating universe and a cosmological constant, *Astron. J.* **116**, 1009 (1998), arXiv:astro-ph/9805201 [astro-ph].
 - [2] S. Perlmutter *et al.* (Supernova Cosmology Project), Measurements of Omega and Lambda from 42 high redshift supernovae, *Astrophys. J.* **517**, 565 (1999), arXiv:astro-ph/9812133 [astro-ph].
 - [3] N. Aghanim *et al.* (Planck), Planck 2018 results. VI. Cosmological parameters, *Astron. Astrophys.* **641**, A6 (2020), arXiv:1807.06209 [astro-ph.CO].
 - [4] P. Ade *et al.* (Planck), Planck 2015 results. XIV. Dark energy and modified gravity, *Astron. Astrophys.* **594**, A14 (2016), arXiv:1502.01590 [astro-ph.CO].
 - [5] P. Bull *et al.*, Beyond Λ CDM: Problems, solutions, and the road ahead, *Phys. Dark Univ.* **12**, 56 (2016), arXiv:1512.05356 [astro-ph.CO].
 - [6] J. Martin, Everything You Always Wanted To Know About The Cosmological Constant Problem (But Were Afraid To Ask), *Comptes Rendus Physique* **13**, 566 (2012), arXiv:1205.3365 [astro-ph.CO].
 - [7] E. J. Copeland, M. Sami, and S. Tsujikawa, Dynamics of dark energy, *Int. J. Mod. Phys. D* **15**, 1753 (2006), arXiv:hep-th/0603057.
 - [8] L. Amendola and S. Tsujikawa, *Dark energy: theory and observations* (Cambridge University Press, 2010).
 - [9] A. G. Riess, L. Macri, S. Casertano, H. Lampeitl, H. C. Ferguson, A. V. Filippenko, S. W. Jha, W. Li, and R. Chornock, A 3% Solution: Determination of the Hubble Constant with the Hubble Space Telescope and Wide Field Camera 3, *Astrophys. J.* **730**, 119 (2011), [Erratum: *Astrophys.J.* 732, 129 (2011)], arXiv:1103.2976 [astro-ph.CO].
 - [10] A. G. Riess *et al.*, A 2.4% Determination of the Local Value of the Hubble Constant, *Astrophys. J.* **826**, 56 (2016), arXiv:1604.01424 [astro-ph.CO].
 - [11] A. G. Riess *et al.*, Milky Way Cepheid Standards for Measuring Cosmic Distances and Application to Gaia DR2: Implications for the Hubble Constant, *Astrophys. J.* **861**, 126 (2018), arXiv:1804.10655 [astro-ph.CO].
 - [12] E. Di Valentino *et al.*, Snowmass2021 - Letter of interest cosmology intertwined II: The hubble constant tension, *Astropart. Phys.* **131**, 102605 (2021), arXiv:2008.11284 [astro-ph.CO].
 - [13] H. Hildebrandt *et al.*, KiDS-450: Cosmological parameter constraints from tomographic weak gravitational lensing, *Mon. Not. Roy. Astron. Soc.* **465**, 1454 (2017), arXiv:1606.05338 [astro-ph.CO].
 - [14] K. Kuijken *et al.*, Gravitational Lensing Analysis of the Kilo Degree Survey, *Mon. Not. Roy. Astron. Soc.* **454**, 3500 (2015), arXiv:1507.00738 [astro-ph.CO].
 - [15] I. Fenech Conti, R. Herbonnet, H. Hoekstra, J. Merten, L. Miller, and M. Viola, Calibration of weak-lensing shear in the Kilo-Degree Survey, *Mon. Not. Roy. Astron. Soc.* **467**, 1627 (2017), arXiv:1606.05337 [astro-ph.CO].
 - [16] E. Di Valentino and S. Bridle, Exploring the Tension between Current Cosmic Microwave Background and Cosmic Shear Data, *Symmetry* **10**, 585 (2018).
 - [17] E. Di Valentino *et al.*, Cosmology intertwined III: $f\sigma_8$ and S_8 , *Astropart. Phys.* **131**, 102604 (2021), arXiv:2008.11285 [astro-ph.CO].
 - [18] A. G. Riess, S. Casertano, W. Yuan, L. M. Macri, and D. Scolnic, Large Magellanic Cloud Cepheid Standards Provide a 1% Foundation for the Determination of the Hubble Constant and Stronger Evidence for Physics beyond Λ CDM, *Astrophys. J.* **876**, 85 (2019), arXiv:1903.07603 [astro-ph.CO].
 - [19] Z. Davari, V. Marra, and M. Malekjani, Cosmological constrains on minimally and non-minimally coupled scalar field models, *Mon. Not. Roy. Astron. Soc.* **491**, 1920 (2020), arXiv:1911.00209 [gr-qc].
 - [20] E. Di Valentino, A. Melchiorri, and J. Silk, Cosmological hints of modified gravity?, *Phys. Rev. D* **93**, 023513 (2016), arXiv:1509.07501 [astro-ph.CO].
 - [21] J. Solà Peracaula, A. Gomez-Valent, J. de Cruz Pérez, and C. Moreno-Pulido, Brans–Dicke Gravity with a Cosmological Constant Smoothes Out Λ CDM Tensions, *Astrophys. J. Lett.* **886**, L6 (2019), arXiv:1909.02554 [astro-ph.CO].
 - [22] J. Sola, A. Gomez-Valent, J. d. C. Perez, and C. Moreno-Pulido, Brans-Dicke cosmology with a Λ -term: a possible solution to Λ CDM tensions, *Class. Quant. Grav.* **37**, 245003 (2020), arXiv:2006.04273 [astro-ph.CO].
 - [23] A. Joyce, B. Jain, J. Khoury, and M. Trodden, Beyond the Cosmological Standard Model, *Phys. Rept.* **568**, 1 (2015), arXiv:1407.0059 [astro-ph.CO].
 - [24] K. Koyama, Cosmological Tests of Modified Gravity, *Rept. Prog. Phys.* **79**, 046902 (2016), arXiv:1504.04623 [astro-ph.CO].
 - [25] C. Wetterich, Cosmology and the Fate of Dilatation Symmetry, *Nucl. Phys. B* **302**, 668 (1988), arXiv:1711.03844 [hep-th].
 - [26] B. Ratra and P. Peebles, Cosmological Consequences of a Rolling Homogeneous Scalar Field, *Phys. Rev. D* **37**, 3406 (1988).
 - [27] S. M. Carroll, Quintessence and the rest of the world, *Phys. Rev. Lett.* **81**, 3067 (1998), arXiv:astro-ph/9806099.
 - [28] S. Tsujikawa, Quintessence: A Review, *Class. Quant.*

- Grav. **30**, 214003 (2013), arXiv:1304.1961 [gr-qc].
- [29] T. Chiba, T. Okabe, and M. Yamaguchi, Kinetically driven quintessence, Phys. Rev. D **62**, 023511 (2000), arXiv:astro-ph/9912463.
- [30] C. Armendariz-Picon, V. F. Mukhanov, and P. J. Steinhardt, A Dynamical solution to the problem of a small cosmological constant and late time cosmic acceleration, Phys. Rev. Lett. **85**, 4438 (2000), arXiv:astro-ph/0004134.
- [31] C. Armendariz-Picon, V. F. Mukhanov, and P. J. Steinhardt, Essentials of k essence, Phys. Rev. D **63**, 103510 (2001), arXiv:astro-ph/0006373.
- [32] A. Sen, Rolling tachyon, JHEP **04**, 048, arXiv:hep-th/0203211.
- [33] A. Sen, Tachyon matter, JHEP **07**, 065, arXiv:hep-th/0203265.
- [34] A. D. Linde, Coleman-Weinberg Theory and a New Inflationary Universe Scenario, Phys. Lett. B **114**, 431 (1982).
- [35] D. Z. Freedman, I. J. Muzinich, and E. J. Weinberg, On the Energy-Momentum Tensor in Gauge Field Theories, Annals Phys. **87**, 95 (1974).
- [36] D. Z. Freedman and E. J. Weinberg, The Energy-Momentum Tensor in Scalar and Gauge Field Theories, Annals Phys. **87**, 354 (1974).
- [37] N. D. Birrell and P. C. W. Davies, *Quantum Fields in Curved Space* (Cambridge Univ. Press, Cambridge, UK, 1984).
- [38] F. Perrotta, C. Baccigalupi, and S. Matarrese, Extended quintessence, Phys. Rev. D **61**, 023507 (1999), arXiv:astro-ph/9906066.
- [39] V. Sahni and S. Habib, Does inflationary particle production suggest Omega(m) less than 1?, Phys. Rev. Lett. **81**, 1766 (1998), arXiv:hep-ph/9808204.
- [40] T. Chiba, Quintessence, the gravitational constant, and gravity, Phys. Rev. D **60**, 083508 (1999), arXiv:gr-qc/9903094.
- [41] N. Bartolo and M. Pietroni, Scalar tensor gravity and quintessence, Phys. Rev. D **61**, 023518 (2000), arXiv:hep-ph/9908521.
- [42] V. Faraoni, Inflation and quintessence with nonminimal coupling, Phys. Rev. D **62**, 023504 (2000), arXiv:gr-qc/0002091 [gr-qc].
- [43] O. Hrycyna and M. Szydlowski, Non-minimally coupled scalar field cosmology on the phase plane, JCAP **04**, 026, arXiv:0812.5096 [hep-th].
- [44] O. Hrycyna and M. Szydlowski, Extended Quintessence with non-minimally coupled phantom scalar field, Phys. Rev. D **76**, 123510 (2007), arXiv:0707.4471 [hep-th].
- [45] A. A. Sen and N. Devi, Cosmology With Non-Minimally Coupled K-Field, Gen. Rel. Grav. **42**, 821 (2010), arXiv:0809.2852 [astro-ph].
- [46] R. C. de Souza and G. M. Kremer, Constraining non-minimally coupled tachyon fields by Noether symmetry, Class. Quant. Grav. **26**, 135008 (2009), arXiv:0809.2331 [gr-qc].
- [47] C. Deffayet, G. Esposito-Farese, and A. Vikman, Covariant Galileon, Phys. Rev. D **79**, 084003 (2009), arXiv:0901.1314 [hep-th].
- [48] E. Di Valentino, A. Melchiorri, O. Mena, and S. Vagnozzi, Nonminimal dark sector physics and cosmological tensions, Phys. Rev. D **101**, 063502 (2020), arXiv:1910.09853 [astro-ph.CO].
- [49] A. Einstein, Riemannian geometry with maintaining the notion of distant parallelism, Sitz. Preuss. Akad. Wiss **217** (1928).
- [50] A. Unzicker and T. Case, Translation of einstein's attempt of a unified field theory with teleparallelism, arXiv:physics/0503046 (2005).
- [51] A. Einstein, A theory of gravitation, Math. Ann. **102**, 685 (1930).
- [52] A. Einstein, A theory of gravitation, Sitzungsber. Preuss. Akad. Wiss. Phys. Math. Kl. **401** (1930).
- [53] C. Pellegrini and J. Plebanski, A theory of gravitation, Math.-Fys. Skr. Dan. Vid. Selskab **2** (1962).
- [54] C. Møller, On the crisis in the theory of gravitation and a possible solution, K. Dan. Vidensk. Selsk., Mat.-Fys. Medd **39**, 1 (1978).
- [55] K. Hayashi and T. Nakano, Extended translation invariance and associated gauge fields, Progress of Theoretical Physics **38**, 491 (1967).
- [56] K. Hayashi and T. Shirafuji, New general relativity, Phys. Rev. D **19**, 3524 (1979).
- [57] J. G. Pereira, Teleparallelism: A New Insight Into Gravity, in *Handbook of Spacetime*, edited by A. Ashtekar and V. Petkov (Springer, 2014) pp. 197–212, 1302.6983 [gr-qc].
- [58] V. C. de Andrade, L. C. T. Guillen, and J. G. Pereira, Gravitational energy momentum density in teleparallel gravity, Phys. Rev. Lett. **84**, 4533 (2000), arXiv:gr-qc/0003100 [gr-qc].
- [59] H. I. Arcos and J. G. Pereira, Torsion gravity: A Reappraisal, Int. J. Mod. Phys. D **13**, 2193 (2004), arXiv:gr-qc/0501017 [gr-qc].
- [60] J. G. Pereira and Y. N. Obukhov, Gauge Structure of Teleparallel Gravity, *Proceedings, Teleparallel Universes in Salamanca: Salamanca, Spain, November 26–28, 2018*, Universe **5**, 139 (2019), arXiv:1906.06287 [gr-qc].
- [61] R. Aldrovandi and J. G. Pereira, *Teleparallel gravity: an introduction*, Vol. 173 (Springer Science & Business Media, 2012).
- [62] Y.-F. Cai, S. Capozziello, M. De Laurentis, and E. N. Saridakis, f(T) teleparallel gravity and cosmology, Rept. Prog. Phys. **79**, 106901 (2016), arXiv:1511.07586 [gr-qc].
- [63] S. Bahamonde, C. G. Böhmer, S. Carloni, E. J. Copeland, W. Fang, and N. Tamanini, Dynamical systems applied to cosmology: dark energy and modified gravity, Phys. Rept. **775–777**, 1 (2018), arXiv:1712.03107 [gr-qc].
- [64] C.-Q. Geng, C.-C. Lee, E. N. Saridakis, and Y.-P. Wu, Teleparallel dark energy, Phys. Lett. B **704**, 384 (2011), arXiv:1109.1092 [hep-th].
- [65] C.-Q. Geng, C.-C. Lee, and E. N. Saridakis, Observational Constraints on Teleparallel Dark Energy, JCAP **1201**, 002, arXiv:1110.0913 [astro-ph.CO].
- [66] G. Otalora, Scaling attractors in interacting teleparallel dark energy, JCAP **1307**, 044, arXiv:1305.0474 [gr-qc].
- [67] G. Otalora, Cosmological dynamics of tachyonic teleparallel dark energy, Phys. Rev. D **88**, 063505 (2013), arXiv:1305.5896 [gr-qc].
- [68] G. R. Bengochea and R. Ferraro, Dark torsion as the cosmic speed-up, Phys. Rev. D **79**, 124019 (2009), arXiv:0812.1205 [astro-ph].
- [69] E. V. Linder, Einstein's Other Gravity and the Acceleration of the Universe, Phys. Rev. D **81**, 127301 (2010), arXiv:1005.3039 [astro-ph.CO].

- [70] B. Li, T. P. Sotiriou, and J. D. Barrow, Large-scale Structure in f(T) Gravity, Phys. Rev. D **83**, 104017 (2011), arXiv:1103.2786 [astro-ph.CO].
- [71] T. Harko, F. S. N. Lobo, G. Otalora, and E. N. Saridakis, $f(T, \mathcal{T})$ gravity and cosmology, JCAP **12**, 021, arXiv:1405.0519 [gr-qc].
- [72] T. Harko, F. S. N. Lobo, G. Otalora, and E. N. Saridakis, Nonminimal torsion-matter coupling extension of f(T) gravity, Phys. Rev. D **89**, 124036 (2014), arXiv:1404.6212 [gr-qc].
- [73] S. Carloni, F. S. Lobo, G. Otalora, and E. N. Saridakis, Dynamical system analysis for a nonminimal torsion-matter coupled gravity, Phys. Rev. D **93**, 024034 (2016), arXiv:1512.06996 [gr-qc].
- [74] M. Gonzalez-Espinoza, G. Otalora, J. Saavedra, and N. Videla, Growth of matter overdensities in non-minimal torsion-matter coupling theories, Eur. Phys. J. C **78**, 799 (2018), arXiv:1808.01941 [gr-qc].
- [75] S. Nojiri and S. D. Odintsov, Gravity assisted dark energy dominance and cosmic acceleration, Phys. Lett. B **599**, 137 (2004), arXiv:astro-ph/0403622.
- [76] G. Allemandi, A. Borowiec, M. Francaviglia, and S. D. Odintsov, Dark energy dominance and cosmic acceleration in first order formalism, Phys. Rev. D **72**, 063505 (2005), arXiv:gr-qc/0504057.
- [77] S. Nojiri and S. D. Odintsov, Introduction to modified gravity and gravitational alternative for dark energy, eConf **C0602061**, 06 (2006), arXiv:hep-th/0601213.
- [78] O. Bertolami, C. G. Boehmer, T. Harko, and F. S. Lobo, Extra force in f(R) modified theories of gravity, Phys. Rev. D **75**, 104016 (2007), arXiv:0704.1733 [gr-qc].
- [79] T. Harko, Modified gravity with arbitrary coupling between matter and geometry, Phys. Lett. B **669**, 376 (2008), arXiv:0810.0742 [gr-qc].
- [80] T. Harko and F. S. Lobo, f(R, L_m) gravity, Eur. Phys. J. C **70**, 373 (2010), arXiv:1008.4193 [gr-qc].
- [81] O. Bertolami and J. Paramos, Mimicking dark matter through a non-minimal gravitational coupling with matter, JCAP **03**, 009, arXiv:0906.4757 [astro-ph.GA].
- [82] O. Bertolami, P. Frazão, and J. Páramos, Cosmological perturbations in theories with non-minimal coupling between curvature and matter, JCAP **05**, 029, arXiv:1303.3215 [gr-qc].
- [83] J. Wang and H. Wang, Evolution of matter density perturbations in f(R) theories of gravity with non-minimal coupling between matter and geometry, Phys. Lett. B **724**, 5 (2013).
- [84] N. D. Birrell, N. D. Birrell, P. Davies, and P. Davies, *Quantum fields in curved space* (Cambridge university press, 1984).
- [85] M. Gonzalez-Espinoza and G. Otalora, Generating primordial fluctuations from modified teleparallel gravity with local Lorentz-symmetry breaking, Phys. Lett. B **809**, 135696 (2020), arXiv:2005.03753 [gr-qc].
- [86] M. Gonzalez-Espinoza and G. Otalora, Cosmological dynamics of dark energy in scalar-torsion $f(T, \phi)$ gravity, Eur. Phys. J. C **81**, 480 (2021), arXiv:2011.08377 [gr-qc].
- [87] M. Gonzalez-Espinoza, G. Otalora, Y. Leyva, and J. Saavedra, Dynamics of dark energy in a scalar-vector-torsion theory, Eur. Phys. J. Plus **138**, 600 (2023), arXiv:2212.12071 [gr-qc].
- [88] M. Gonzalez-Espinoza, G. Otalora, Y. Leyva, and J. Saavedra, Phase-space analysis of torsion-coupled dilatonic ghost condensate, (2023), arXiv:2306.03386 [gr-qc].
- [89] J.-P. Uzan, Cosmological scaling solutions of nonminimally coupled scalar fields, Phys. Rev. D **59**, 123510 (1999), arXiv:gr-qc/9903004.
- [90] L. Amendola, Scaling solutions in general nonminimal coupling theories, Phys. Rev. D **60**, 043501 (1999), arXiv:astro-ph/9904120.
- [91] S. A. Kadam, L. K. Duchaniya, and B. Mishra, Teleparallel Gravity and Quintessence: The Role of Nonminimal Boundary Couplings, arXiv (2024), arXiv:2408.03417 [gr-qc].
- [92] S. A. Kadam, A. Sahu, S. K. Tripathy, and B. Mishra, Dynamical System Analysis for Scalar Field Potential in Teleparallel Gravity, arXiv (2024), arXiv:2405.10354 [gr-qc].
- [93] S. A. Kadam, N. P. Thakkar, and B. Mishra, Dynamical system analysis in teleparallel gravity with boundary term, Eur. Phys. J. C **83**, 809 (2023), arXiv:2306.06677 [gr-qc].
- [94] L. K. Duchaniya, K. Gandhi, and B. Mishra, Attractor behavior of f(T) modified gravity and the cosmic acceleration, Phys. Dark Univ. **44**, 101461 (2024), arXiv:2303.09076 [gr-qc].
- [95] A. De Felice, N. Frusciante, and G. Papadomanolakis, On the stability conditions for theories of modified gravity in the presence of matter fields, JCAP **1703**, 027, arXiv:1609.03599 [gr-qc].
- [96] L. Heisenberg, R. Kase, and S. Tsujikawa, Beyond generalized Proca theories, Phys. Lett. B **760**, 617 (2016), arXiv:1605.05565 [hep-th].
- [97] R. Kase and S. Tsujikawa, Effective field theory approach to modified gravity including Horndeski theory and Hořava–Lifshitz gravity, Int. J. Mod. Phys. D **23**, 1443008 (2015), arXiv:1409.1984 [hep-th].
- [98] A. De Felice and S. Tsujikawa, Conditions for the cosmological viability of the most general scalar-tensor theories and their applications to extended Galileon dark energy models, JCAP **02**, 007, arXiv:1110.3878 [gr-qc].
- [99] F. Sbisà, Classical and quantum ghosts, Eur. J. Phys. **36**, 015009 (2015), arXiv:1406.4550 [hep-th].
- [100] L. A. Gergely and S. Tsujikawa, Effective field theory of modified gravity with two scalar fields: dark energy and dark matter, Phys. Rev. D **89**, 064059 (2014), arXiv:1402.0553 [hep-th].
- [101] J. Gleyzes, D. Langlois, F. Piazza, and F. Vernizzi, Exploring gravitational theories beyond Horndeski, JCAP **02**, 018, arXiv:1408.1952 [astro-ph.CO].
- [102] B. Wang, E. Abdalla, F. Atrio-Barandela, and D. Pavon, Dark matter and dark energy interactions: theoretical challenges, cosmological implications and observational signatures, Reports on Progress in Physics **79**, 096901 (2016).
- [103] B. Wang, E. Abdalla, F. Atrio-Barandela, and D. Pavon, Further understanding the interaction between dark energy and dark matter: current status and future directions, Reports on Progress in Physics (2024).
- [104] C. Rodriguez-Benites, M. Gonzalez-Espinoza, G. Otalora, and M. Alva-Morales, Revisiting the dynamics of interacting vector-like dark energy, The European Physical Journal C **84**, 276 (2024).
- [105] C. Rodriguez-Benites, M. Cataldo, and M. Vásquez-Arteaga, Universe with holographic dark energy, Mo-

- mento , 1 (2020).
- [106] A. Cid, C. Rodriguez-Benites, M. Cataldo, and G. Casanova, Bayesian Comparison of Interacting Modified Holographic Ricci Dark Energy Scenarios, *Eur. Phys. J. C* **81**, 31 (2021), arXiv:2005.07664 [astro-ph.CO].
- [107] L. Amendola and S. Tsujikawa, Scaling solutions and weak gravity in dark energy with energy and momentum couplings, *Journal of Cosmology and Astroparticle Physics* **2020** (06), 020.
- [108] J. B. Jiménez, D. Bettoni, D. Figueruelo, F. A. T. Pannia, and S. Tsujikawa, Velocity-dependent interacting dark energy and dark matter with a lagrangian description of perfect fluids, *Journal of Cosmology and Astroparticle Physics* **2021** (03), 085.
- [109] J. Beltrán Jiménez, D. Bettoni, D. Figueruelo, F. A. Teppa Pannia, and S. Tsujikawa, Probing elastic interactions in the dark sector and the role of s 8, *Physical Review D* **104**, 103503 (2021).
- [110] J. B. Jiménez, E. Di Dio, and D. Figueruelo, A smoking gun from the power spectrum dipole for elastic interactions in the dark sector, *Journal of Cosmology and Astroparticle Physics* **2023** (11), 088.
- [111] J. B. Jiménez, D. Bettoni, D. Figueruelo, and F. A. T. Pannia, On cosmological signatures of baryons-dark energy elastic couplings, *Journal of Cosmology and Astroparticle Physics* **2020** (08), 020.
- [112] M. Asghari, J. B. Jiménez, S. Khosravi, and D. F. Mota, On structure formation from a small-scales-interacting dark sector, *Journal of Cosmology and Astroparticle Physics* **2019** (04), 042.
- [113] B. F. Schutz and R. Sorkin, Variational aspects of relativistic field theories, with application to perfect fluids, *Annals Phys.* **107**, 1 (1977).
- [114] J. Brown, Action functionals for relativistic perfect fluids, *Class. Quant. Grav.* **10**, 1579 (1993), arXiv:gr-qc/9304026.
- [115] M. Gonzalez-Espinoza, G. Otalora, and J. Saavedra, Stability of scalar perturbations in scalar-torsion $f(T, \phi)$ gravity theories in the presence of a matter fluid, *JCAP* **10**, 007, arXiv:2101.09123 [gr-qc].
- [116] G. Otalora, A novel teleparallel dark energy model, *Int. J. Mod. Phys. D* **25**, 1650025 (2015), arXiv:1402.2256 [gr-qc].
- [117] M. A. Skugoreva, E. N. Saridakis, and A. V. Toporenko, Dynamical features of scalar-torsion theories, *Phys. Rev. D* **91**, 044023 (2015), arXiv:1412.1502 [gr-qc].
- [118] M. Hohmann, L. Järv, and U. Ulalikhanova, Covariant formulation of scalar-torsion gravity, *Phys. Rev. D* **97**, 104011 (2018), arXiv:1801.05786 [gr-qc].
- [119] L. Amendola and S. Tsujikawa, Scaling solutions and weak gravity in dark energy with energy and momentum couplings, *JCAP* **06**, 020, arXiv:2003.02686 [gr-qc].
- [120] M. Gonzalez-Espinoza, R. Herrera, G. Otalora, and J. Saavedra, Reconstructing inflation in scalar-torsion $f(T, \phi)$ gravity, *Eur. Phys. J. C* **81**, 731 (2021), arXiv:2106.06145 [gr-qc].
- [121] P. G. Ferreira and M. Joyce, Cosmology with a primordial scaling field, *Phys. Rev. D* **58**, 023503 (1998), arXiv:astro-ph/9711102.
- [122] R. Bean, S. H. Hansen, and A. Melchiorri, Early universe constraints on a primordial scaling field, *Phys. Rev. D* **64**, 103508 (2001), arXiv:astro-ph/0104162.
- [123] S.-L. Cao, X.-W. Duan, X.-L. Meng, and T.-J. Zhang, Cosmological model-independent test of \varlambda cdm with two-point diagnostic by the observational hubble parameter data, *The European Physical Journal C* **78**, 1 (2018).
- [124] O. Farooq and B. Ratra, Hubble parameter measurement constraints on the cosmological deceleration-acceleration transition redshift, *The Astrophysical Journal Letters* **766**, L7 (2013).
- [125] C. Zhang, H. Zhang, S. Yuan, S. Liu, T.-J. Zhang, and Y.-C. Sun, Four new observational h (z) data from luminous red galaxies in the Sloan Digital Sky Survey data release seven, *Res. Astron. Astrophys.* **14**, 1221 (2014).
- [126] J. Simon, L. Verde, and R. Jimenez, Constraints on the redshift dependence of the dark energy potential, *Phys. Rev. D* **71**, 123001 (2005).
- [127] M. Moresco, A. Cimatti, R. Jimenez, L. Pozzetti, G. Zamorani, M. Bolzonella, J. Dunlop, F. Lamareille, M. Mignoli, H. Pearce, et al., Improved constraints on the expansion rate of the universe up to z 1.1 from the spectroscopic evolution of cosmic chronometers, *J. Cosmol. Astropart. Phys.* **2012** (08), 006.
- [128] A. J. Cuesta, M. Vargas-Magaña, F. Beutler, A. S. Bolton, J. R. Brownstein, D. J. Eisenstein, H. Gil-Marín, S. Ho, C. K. McBride, C. Maraston, et al., The clustering of galaxies in the SDSS-III Baryon Oscillation Spectroscopic Survey: Baryon acoustic oscillations in the correlation function of lowz and cmass galaxies in data release 12, *Mon. Not. R. Astron. Soc.* **457**, 1770 (2016).
- [129] C. Blake, S. Brough, M. Colless, C. Contreras, W. Couch, S. Croom, D. Croton, T. M. Davis, M. J. Drinkwater, K. Forster, et al., The WiggleZ dark energy survey: Joint measurements of the expansion and growth history at z 1, *Mon. Not. R. Astron. Soc.* **425**, 405 (2012).
- [130] A. Ratsimbazafy, S. Loubser, S. Crawford, C. Cress, B. Bassett, R. Nichol, and P. Väistönen, Age-dating luminous red galaxies observed with the southern African Large Telescope, *Mon. Not. R. Astron. Soc.* **467**, 3239 (2017).
- [131] D. Stern, R. Jimenez, L. Verde, M. Kamionkowski, and S. A. Stanford, Cosmic chronometers: constraining the equation of state of dark energy. i: H (z) measurements, *J. Cosmol. Astropart. Phys.* **2010** (02), 008.
- [132] M. Moresco, Raising the bar: new constraints on the hubble parameter with cosmic chronometers at z ~ 2, *Mon. Not. R. Astron. Soc.* **450**, L16 (2015).
- [133] T. Delubac, J. E. Bautista, J. Rich, D. Kirkby, S. Bailey, A. Font-Ribera, A. Slosar, K.-G. Lee, M. M. Pieri, J.-C. Hamilton, et al., Baryon acoustic oscillations in the Lyα forest of BOSS DR11 quasars, *A&A* **574**, 59 (2015).
- [134] A. Font-Ribera, D. Kirkby, J. Miralda-Escudé, N. P. Ross, A. Slosar, J. Rich, É. Aubourg, S. Bailey, V. Bhardwaj, J. Bautista, et al., Quasar-Lyman α forest cross-correlation from BOSS DR11: Baryon acoustic oscillations, *J. Cosmol. Astropart. Phys.* **2014** (05), 027.

Appendix A: Properties of critical points

The properties of the critical points of the autonomous system (45) are shown in Table III, where the following set of definitions has been made:

- For point c_R

$$\beta_{1,c} = \frac{1}{4}(-2 + 3Q^2), \quad \beta_{2,c} = \frac{1}{4}(-1 + 2Q^2).$$

- For point d_M

$$\begin{aligned}\beta_{d,1} &= \frac{1}{2}(-1 + 2Q^2), \quad \beta_{d,2} = \frac{1}{2}(-1 - 2Q^2), \\ \lambda_{d,1} &= \frac{-4 - 6\beta}{\sqrt{2}}, \quad \lambda_{d,2} = \frac{-3 - 2Q^2 - 6\beta}{2Q}.\end{aligned}$$

- For point e^\pm

$$\beta_{1,e} = \frac{1}{12}(-6 + \lambda^2), \quad \beta_{2,e} = \frac{1}{6}(-3 + 2Q^2).$$

- For point f_R

$$\beta_{f,1} = \frac{1}{128}(-64 + 15\lambda^2), \quad \beta_{f,2} = \frac{1}{8}(-4 + \lambda^2).$$

- For point g

$$\begin{aligned}\beta_{1,g} &= \frac{1}{12}(-6 + \lambda^2), \quad \beta_{2,g} = \frac{1}{4}(-2 + \lambda^2), \\ Q_{1,g} &= \frac{3 + 6\beta - \lambda^2}{\lambda}.\end{aligned}$$

- For point h

$$\beta_{h,0} = \frac{1}{6}(-3 - 2Q^2 - 2Q\lambda),$$

$$\beta_{h,1} = \frac{1}{96}(-48 - 20Q^2 - 12Q\lambda + 7\lambda^2) - \frac{R_f}{96},$$

$$\beta_{h,2} = \frac{1}{6}(-3 - 2Q^2 - 2Q\lambda) - \frac{R_f}{96},$$

$$\beta_{h,3} = \frac{1}{96}(-48 - 20Q^2 - 12Q\lambda + 7\lambda^2) + \frac{R_f}{96},$$

$$\beta_{h,4} = \frac{1}{6}(-3 + Q\lambda + \lambda^2).$$

where

$$R_f = \sqrt{400Q^4 + 992Q^3\lambda + 888Q^2\lambda^2 + 344Q\lambda^3 + 49\lambda^4}.$$

Table III. Properties of the critical points

Name	Existence	Stability	Acceleration
a_R	$\forall \lambda, \sigma, Q, \beta$	unstable $\forall \lambda, \sigma, Q, \beta$	never
b	$(\sigma < 0 \wedge (\lambda < 0 \vee 0 < \lambda < -\sigma))$ $\vee (\sigma > 0 \wedge (-\sigma < \lambda < 0 \vee \lambda > 0))$	$(\sigma < 0 \wedge ((\beta < -\frac{1}{2} \wedge \frac{-6\beta-3}{4\sigma} \leq \lambda < 0) \vee (\beta > -\frac{1}{2} \wedge 0 < \lambda \leq \frac{-6\beta-3}{4\sigma})))$ $\vee (\sigma > 0 \wedge ((\beta < -\frac{1}{2} \wedge 0 < \lambda \leq \frac{-6\beta-3}{4\sigma}) \vee (\beta > -\frac{1}{2} \wedge \frac{-6\beta-3}{4\sigma} \leq \lambda < 0)))$	always
c_R	$(Q < 0 \wedge -\frac{1}{2} < \beta < \frac{1}{2} (2Q^2 - 1))$ $\vee (Q > 0 \wedge -\frac{1}{2} < \beta < \frac{1}{2} (2Q^2 - 1))$	$(\lambda < 0 \wedge 0 < Q < -\frac{\lambda}{4} \wedge \beta_{1,c} \leq \beta < \beta_{2,c} \wedge \sigma < 0) \vee (\lambda > 0 \wedge -\frac{\lambda}{4} < Q < 0 \wedge \beta_{1,c} \leq \beta < \beta_{2,c} \wedge \sigma > 0)$	never
d_M	$(Q < 0 \wedge \beta > \frac{1}{6} (2Q^2 - 3))$ $\vee (Q > 0 \wedge \beta > \frac{1}{6} (2Q^2 - 3))$	$(Q < -\frac{1}{\sqrt{2}} \wedge ((\beta < -\frac{1}{2} \wedge \lambda < \lambda_{d,2} \wedge \sigma < 0) \vee (\beta > \beta_{d,1} \wedge \lambda > \lambda_{d,2} \wedge \sigma > 0))) \vee (Q = -\frac{1}{\sqrt{2}} \wedge ((\beta < -\frac{1}{2} \wedge \lambda < -\lambda_{d,1} \wedge \sigma > 0) \vee (-\frac{1}{\sqrt{2}} < Q < 0 \wedge ((\beta < -\frac{1}{2} \wedge \lambda < \lambda_{d,2} \wedge \sigma > 0) \vee (0 < Q < \frac{1}{\sqrt{2}} \wedge ((\beta < -\frac{1}{2} \wedge \lambda > \lambda_{d,2} \wedge \sigma > 0) \vee (\beta > \beta_{d,1} \wedge \lambda < \lambda_{d,2} \wedge \sigma < 0)))) \vee (Q = \frac{1}{\sqrt{2}} \wedge ((\beta < -\frac{1}{2} \wedge \lambda > \lambda_{d,1} \wedge \sigma > 0) \vee (\beta > 0 \wedge \lambda < \lambda_{d,1} \wedge \sigma < 0))) \vee (Q > \frac{1}{\sqrt{2}} \wedge ((\beta < -\frac{1}{2} \wedge \lambda > \lambda_{d,2} \wedge \sigma > 0) \vee (\beta > \beta_{d,1} \wedge \lambda < \lambda_{d,2} \wedge \sigma < 0)))$	$(Q < 0 \wedge \beta_{d,2} < \beta < -\frac{1}{2})$ $\vee (Q > 0 \wedge \beta_{d,2} < \beta < -\frac{1}{2})$
e^\pm	$\beta > -\frac{1}{2}$	unstable for $(Q > 0 \wedge ((\beta > -\frac{1}{2} \wedge \lambda < 0 \wedge \sigma < 0) \vee (\lambda > 0 \wedge \beta > \beta_{1,e} \wedge \sigma < 0))) \vee (Q < 0 \wedge \beta > \beta_{2,e} \wedge \lambda < 0 \wedge \sigma < 0) \vee (\lambda > 0 \wedge ((Q \leq -\frac{\lambda}{2} \wedge \beta > \beta_{2,e}) \vee (-\frac{\lambda}{2} < Q < 0 \wedge \beta > \beta_{1,e})) \wedge \sigma < 0)$	never
f_R	$(\lambda < 0 \wedge -\frac{1}{2} < \beta < \frac{1}{8} (\lambda^2 - 4))$ $\vee (\lambda > 0 \wedge -\frac{1}{2} < \beta < \frac{1}{8} (\lambda^2 - 4))$	$(\lambda < 0 \wedge Q > -\frac{\lambda}{4} \wedge \beta_{f,1} \leq \beta < \beta_{f,2} \wedge \sigma < 0) \vee (\lambda > 0 \wedge Q < -\frac{\lambda}{4} \wedge \beta_{f,1} \leq \beta < \beta_{f,2} \wedge \sigma > 0)$	never
g	$(\lambda < 0 \wedge (\beta < -\frac{1}{2} \vee \beta \geq \beta_{1,g}))$ $\vee (\lambda > 0 \wedge (\beta < -\frac{1}{2} \vee \beta \geq \beta_{1,g}))$	$(\lambda < 0 \wedge ((\beta < -\frac{1}{2} \wedge Q < Q_{1,g} \wedge \sigma > 0) \vee (\beta > \frac{1}{8} (\lambda^2 - 4) \wedge Q > Q_{1,g} \wedge \sigma < 0))) \vee (\lambda > 0 \wedge ((\beta < -\frac{1}{2} \wedge Q > Q_{1,g} \wedge \sigma < 0) \vee (\beta > \frac{1}{8} (\lambda^2 - 4) \wedge Q < Q_{1,g} \wedge \sigma > 0)))$	$(\lambda < 0 \wedge (\beta < -\frac{1}{2} \vee \beta > \beta_{2,g}))$ $\vee (\lambda > 0 \wedge (\beta < -\frac{1}{2} \vee \beta > \beta_{2,g}))$
h	$(\lambda < 0 \wedge ((Q < 0 \wedge \beta \geq \beta_{h,0}) \vee (0 < Q < -\lambda \wedge \beta \geq \beta_{h,0}) \vee (Q > -\lambda \wedge \beta \geq \beta_{h,0}))) \vee (\lambda > 0 \wedge ((Q < -\lambda \wedge \beta \geq \beta_{h,0}) \vee (-\lambda < Q < 0 \wedge \beta \geq \beta_{h,0}) \vee (Q > 0 \wedge \beta \geq \beta_{h,0})))$	$(\lambda < 0 \wedge ((Q < 0 \wedge ((\beta_{h,1} \leq \beta < \beta_{h,2} \wedge \sigma < 0) \vee (\beta_{h,3} \leq \beta < \beta_{h,4} \wedge \sigma < 0))) \vee (0 < Q < -\frac{\lambda}{4} \wedge ((\beta_{h,2} < \beta \leq \beta_{h,1} \wedge \sigma < 0) \vee (\beta_{h,3} \leq \beta < \beta_{h,4} \wedge \sigma < 0))) \vee (Q > -\lambda \wedge ((\beta_{h,1} \leq \beta < \beta_{h,2} \wedge \sigma > 0) \vee (\beta_{h,4} < \beta \leq \beta_{h,3} \wedge \sigma > 0))) \vee (\lambda > 0 \wedge ((Q < -\lambda \wedge ((\beta_{h,1} \leq \beta < \beta_{h,2} \wedge \sigma < 0) \vee (\beta_{h,4} < \beta \leq \beta_{h,3} \wedge \sigma < 0))) \vee (-\frac{\lambda}{4} < Q < 0 \wedge ((\beta_{h,2} < \beta \leq \beta_{h,1} \wedge \sigma > 0) \vee (\beta_{h,3} \leq \beta < \beta_{h,4} \wedge \sigma > 0))) \vee (\beta_{h,2} < \beta \leq \beta_{h,1} \wedge \sigma > 0) \vee (\beta_{h,3} \leq \beta < \beta_{h,4} \wedge \sigma > 0)))) \vee (Q > 0 \wedge ((\beta_{h,1} \leq \beta < \beta_{h,2} \wedge \sigma > 0) \vee (\beta_{h,3} \leq \beta < \beta_{h,4} \wedge \sigma > 0))))$	$(\lambda < 0 \wedge (Q < \frac{\lambda}{2} \vee Q > -\lambda))$ $\vee (\lambda > 0 \wedge (Q < -\lambda \vee Q > \frac{\lambda}{2}))$
i_M	$(\sigma < 0 \wedge Q > 0) \vee (\sigma > 0 \wedge Q < 0)$	$(\sigma < 0 \wedge ((\beta < -\frac{1}{2} \wedge 0 < Q \leq \frac{6\beta+3}{16\sigma}) \vee (\beta > -\frac{1}{2} \wedge \frac{6\beta+3}{16\sigma} \leq Q < 0))) \vee (\sigma > 0 \wedge ((\beta < -\frac{1}{2} \wedge \frac{6\beta+3}{16\sigma} \leq Q < 0) \vee (\beta > -\frac{1}{2} \wedge 0 < Q \leq \frac{6\beta+3}{16\sigma})))$	never

Appendix B: Hubble's rate analysis

For this analysis, we utilize a dataset consisting of 39 data points for $0.01 < z < 2.360$, as outlined in Table IV.

Table IV. Hubble's parameter vs. redshift & scale factor.

z	$H(z)$ ($\frac{km/s}{Mpc}$)	Ref.
0.07	69 ± 19.6	[125]
0.09	69 ± 12	[126]
0.100	69 ± 12	[126]
0.120	68.6 ± 26.2	[125]
0.170	83 ± 8	[126]
0.179	75 ± 4	[127]
0.199	75 ± 5	[127]
0.200	72.9 ± 29.6	[125]
0.270	77 ± 14	[126]
0.280	88.8 ± 36.6	[125]
0.320	79.2 ± 5.6	[128]
0.352	83 ± 14	[127]
0.3802	83 ± 13.5	[127]
0.400	95 ± 17	[126]
0.4004	77 ± 10.2	[127]
0.4247	87.1 ± 11.2	[127]
0.440	82.6 ± 7.8	[129]
0.4497	92.8 ± 12.9	[127]
0.470	89 ± 50	[130]
0.4783	80.9 ± 9	[127]
0.480	97 ± 62	[131]
0.570	100.3 ± 3.7	[128]
0.593	104 ± 13	[127]
0.600	87.9 ± 6.1	[129]
0.680	92 ± 8	[127]
0.730	97.3 ± 7	[129]
0.781	105 ± 12	[127]
0.875	125 ± 17	[127]
0.880	90 ± 40	[131]
0.900	117 ± 23	[126]
1.037	154 ± 20	[127]
1.300	168 ± 17	[126]
1.363	160 ± 33.6	[132]
1.430	177 ± 18	[126]
1.530	140 ± 14	[126]
1.750	202 ± 40	[126]
1.965	186.5 ± 50.4	[132]
2.340	222 ± 7	[133]
2.360	226 ± 8	[134]